



OPEN

Acute effects of 2.856 GHz and 1.5 GHz microwaves on spatial memory abilities and CREB-related pathways

Shengzhi Tan¹, Hui Wang²✉, Xinping Xu², Li Zhao², Jing Zhang², Ji Dong², Binwei Yao², Haoyu Wang², Yanhui Hao², Hongmei Zhou², Yabing Gao² & Ruiyun Peng²✉

This study aimed to evaluate the acute effects of 2.856 GHz and 1.5 GHz microwaves on spatial memory and cAMP response element binding (CREB)-related pathways. A total of 120 male Wistar rats were divided into four groups: a control group (C); 2.856 GHz microwave exposure group (S group); 1.5 GHz microwave exposure group (L group); and 2.856 and 1.5 GHz cumulative exposure group (SL group). Decreases in spatial memory abilities, changes in EEG, structural injuries, and the downregulation of phosphorylated-Ak strain transforming (p-AKT), phosphorylated-calcium/calmodulin-dependent protein kinase II (p-CaMKII), phosphorylated extracellular signal regulated kinase (p-ERK) and p-CREB was observed 6 h after microwave exposure. Significant differences in the expression of p-CaMKII were found between the S and L groups. The power amplitudes of the EEG waves (θ , δ), levels of structural injuries and the expression of p-AKT, p-CaMK II, p-CREB, and p-ERK1/2 were significantly different in the S and L groups compared to the SL group. Interaction effects between the 2.856 and 1.5 GHz microwaves were found in the EEG and p-CREB changes. Our findings indicated that 2.856 GHz and 1.5 GHz microwave exposure induced a decline in spatial memory, which might be related to p-AKT, p-CaMK II, p-CREB and p-ERK1/2.

The brain is one of the most sensitive organs to electromagnetic radiation^{1–3}. The effects of microwave radiation on spatial learning and memory ability have been reported in many studies^{4,5}, but the mechanisms are not clear. Most studies focused on the biological effects of microwaves at a single frequency. Microwaves with frequencies of 2.856 GHz and 1.5 GHz belong to the S and C bands, respectively, and are widely used in telecommunication, especially radar communication. Microwaves with different frequencies have different electromagnetic properties, which might induce different biological effects. People who operated radars or lived near a radar station are generally exposed to a complex electromagnetic environment of different frequencies. Therefore, in this study, we used two different frequencies (2.856 GHz and 1.5 GHz) of microwaves with the same power density (10 mW/cm²) to determine the properties and accumulative biological effects of the two different microwaves.

The Morris water maze (MWM), as a classic test for spatial learning and memory in rodents, has been widely used to assess microwave radiation-induced impairment of spatial memory^{6–9}. Electroencephalographic (EEG) data are frequently used to assess the effects of microwave exposure on brain bioelectrical activity because of the sensitivity of these scans to immediate changes in neural processes^{10–12}. However, previous studies paid little attention to the acute effects of microwave radiation. Therefore, the present study evaluated the acute and accumulative effects of two different microwave frequencies on learning and memory abilities and bioelectrical activity.

Microstructural observations should not be neglected in investigations of the possible mechanisms. Neurons are the basis for signal transmission and learning and memory development. Microwave radiation induces neural cell apoptosis via the classic mitochondrion-dependent caspase-3 pathway¹³. The hippocampus and cortex are important brain areas for learning and memory abilities. Therefore, it is necessary to observe changes in the neurons in the hippocampus and cortex, especially the occurrence of neuronal apoptosis.

Many studies have shown that cAMP-response element binding protein (CREB) plays an important role in learning and memory processes^{14–16}. CREB is a key transcription factor that regulates the expression and

¹PLA Strategic Support Force Characteristic Medical Center, Beijing, People's Republic of China. ²Department of Experimental Pathology, Beijing Institute of Radiation Medicine, Beijing, People's Republic of China. ✉email: wanghui597bj@163.com; ruiyunpeng18@126.com

activity of genes to alter the function of neurons^{17–19}. CREB is also a connection between several neural function-related pathways. The phosphoinositide 3-kinase (PI3K)/Akt strain transforming (AKT) pathway, calcium/calmodulin-dependent protein kinase II (Ca²⁺/CaMKII) pathway and mitogen-activated protein kinase (MEK)/extracellular signal regulated kinase (ERK) pathway are three key upstream pathways of CREB^{20–22} and regulate the expression of multiple downstream functional proteins in the nervous system. Activation of the PI3K/AKT pathway was observed in neuron-like cells after microwave exposure, and the changes were considered protective responses^{23–25}. The influx of calcium increases after microwave radiation in neuron-like cells²⁶, which suggests that the Ca²⁺/CaMKII pathway participates in microwave bioeffects. Increased ERK phosphorylation is detected in response to extremely low-frequency electromagnetic fields²⁷. However, the relationship between these microwave-sensitive pathways is not clear.

The present study detected the expression levels of AKT, p-AKT, CaMK II, p-CaMK II, CREB, p-CREB, ERK1/2 and p-ERK1/2. We compared the molecular mechanisms between the different frequency microwaves and explored the possible interaction effects between the two frequencies. These findings could contribute to our understanding of the mechanisms of microwave-induced spatial memory impairment. Two different microwave frequencies were considered two different factors. Therefore, a 2 × 2 factorial design was used to evaluate whether an interaction occurred between the frequencies.

Materials and methods

Animals and groups. The Ethics Committee of the Academy of Military Medical Science approved all experimental protocols for animal care, handling and experimentation (IACUC-DWZX-2020-0780), and all experiments were performed in accordance with relevant guidelines and regulations. All the methods were carried out in accordance with the Guide for the Care and Use of Laboratory Animals published by the US National Institutes of Health (NIH Publication No. 85–23, revised 1996). The study was carried out in compliance with the ARRIVE guidelines (<http://www.nc3rs.org.uk/page.asp?id=1357>).

A total of 120 male Wistar rats (weights 200 ± 20 g) (n = 30 per group) were obtained from the Laboratory Animal Center of the Beijing Institute of Radiation Medicine and housed in a specific pathogen-free (SPF)-grade animal facility. All experiments were performed between 8:00 and 15:00.

The 2.856 GHz and 1.5 GHz microwaves lie within the S band and L band, respectively. Therefore, we used the letter “S” to represent the 2.856 GHz exposure group and the letter “L” to represent the 1.5 GHz exposure group. “SL” represented the 2.856 and 1.5 GHz cumulative microwave exposure group. All rats were randomly divided into four groups: (1) the control group (C); (2) the 2.856 GHz microwave exposure group (S); (3) the 1.5 GHz microwave exposure group (L); and (4) the 2.856 and 1.5 GHz cumulative microwave exposure (SL).

Microwave exposure and dosimetry. Two microwave sources with a frequency of 2.856 GHz or 1.5 GHz were placed next to each other in an electromagnetic shield chamber. The exposure procedures were the same as those used by Tan²⁸. Briefly, rats in the S and L groups were exposed to 2.856 GHz or 1.5 GHz microwaves, respectively, with an average power density of 10 mW/cm² for 6 min. Rats in the SL group were first exposed to the 2.856 GHz antenna (the S band) for 6 min then moved parallel to the 1.5 GHz antenna (the L band) for 6 min via a conveyor belt. The interval time between the two exposure procedures was very short and may be negligible.

The specific absorption rate (SAR) values were calculated as described in our previous paper². The SAR values were calculated as described in our previous paper²⁸. The SAR values of the whole body for C, S and L were 0, 3.3 and 3.7 W/kg, respectively. For the SL group, the SAR values of the whole body were 3.3 W/kg for the first 6 min and 3.7 W/kg for the last 6 min.

Morris water maze. The procedures for the Morris water maze strictly followed those of previous reports^{6,29}. Briefly, a circular pool with a diameter of 150 cm was filled with water at 23 ± 0.5 °C in a room with constant brightness and divided into four equal quadrants. A platform with a diameter of 12 cm and a height of 15 cm was submerged 1.5 cm under the water surface. A Morris water maze video analysis system (Beijing Sunny Instrument Co., Ltd., Beijing, China) based on moving object detection and tracking was used.

Sixty male Wistar rats (n = 15 per group) in a fixed order were trained to find the submerged platform in 4 trials before microwave exposure. The training experiment lasted 2 days. The rats were trained to find the submerged escape platform for three consecutive days before the initiation of radiation. Each trial consisted of four trials, which started from four different starting positions. These positions were equally located around the perimeter of the pool and used in a fixed order. Each trial had a maximum duration of 60 s. Rats that did not find the platform within 60 s in the training tests were placed on the platform for 15 s. The rats were exposed to microwave radiation on day 3. Navigation tests were performed 6 h after microwave exposure to detect acute changes in spatial memory. Four trials were conducted, and each trial had a maximum duration of 60 s. The duration of each rat to find the platform was recorded separately, and the average escape latency (AEL) of each rat in the water maze was obtained by calculating the average of 4 trials for each experimental animal for each training day. The behavior of the rats was digitally recorded by using a SLY-MW system (Beijing Sunny Instrument Co., China), and the AEL was analyzed.

EEG recordings. Twenty male Wistar rats (n = 5 per group) were anesthetized with 1% sodium pentobarbital (0.5 ml/100 g). An Mp-150 multichannel physiological recording and analysis system (Biopac Company, USA) was used. The electrodes were connected to the amplifier, and the rats were recorded for 3 min in a quiet state 6 h after microwave exposure. Afterward, power spectral analyses were performed.

Hematoxylin and eosin (H&E) and TUNEL staining of the hippocampus. Twenty male Wistar rats ($n = 5$ per group) were anesthetized with sodium pentobarbital (50 mg/kg, IP) 6 h after microwave exposure. The skin was removed from the head of the anesthetized rats. The bregma point of the brain tissue was marked and drilled, and the brain tissue was separated. The right brain tissue was cut 3.3–3.8 mm behind the bregma point. The brain tissues were fixed in formalin. The right brains were separated and fixed in a 10% buffered formalin solution for at least 1 week. Coronal brain sections, including the hippocampus, were made. The sections were selected at 3.6 mm behind the bregma point. The sections were dried, dewaxed, dipped in hematoxylin for 15 min and washed for 20 min with tap water. Eosin was used to stain the sections for 15 s. Sections were dehydrated in an alcohol gradient and cleared in xylene. Cover slips were placed on the slides, and the stained sections were observed under a Leica DM6000 light microscope (Leica, Germany). The DG area of the hippocampus was observed with a light microscope.

Paraffin sections of the hippocampus were prepared 6 h after microwave exposure. The sections were dried, dewaxed, and treated with proteinase K (20 $\mu\text{g}/\text{ml}$, Roche, Switzerland) for 10 min to make the cell membrane permeable. The sections were then treated with the reaction solution mixture (enzyme solution and label solution, Roche, Switzerland) for the TdT-mediated dUTP nick-end labeling (TUNEL) reaction. After treatment with biotin-labeled horseradish peroxidase (HRP, ZSGB, Beijing, China), 3,3'-diaminobenzidine (DAB) chromogen (ZSGB, Beijing, China) was used to develop the color. A Leica DM6000 light microscope was used to observe the stained sections. The DG areas were selected at 3.6 mm posterior to bregma, 2–2.5 mm lateral to the mid-line and at a depth of approximately 3.5 mm.

Pathological analyses used five rats from each group. Ten sections of each rats were made. Approximately 60 cells in the DG area were selected from each section. The mean optical density (MOD) in H&E sections referred to the ratio of the area of the dark blue nucleus to the total area of the nucleus in the observed cells. The integrated optical density (IOD) referred to the whole optical density of all positive nuclei from observed cells in the TUNEL-stained sections. As for calculating IOD, the background from each section was subtracted and each rat was used for one datapoint.

Western blotting. Twenty male Wistar rats ($n = 5$ per group) were anesthetized, and the entire left hippocampus was separated. The tissue was homogenized for Western blotting (WB). The expression levels of p-AKT, p-CaMKII, p-CREB, p-ERK1/2, AKT, CaMKII, CREB and ERK1/2 in the hippocampi of the rats were detected by WB 6 h after microwave exposure. Protein extraction and quantification and WB procedures were performed according to Xiong's research²⁶. Primary antibodies against p-AKT (Abcam, UK), p-CaMKII (Abcam, UK), p-CREB (Abcam, UK), p-ERK1/2 (Abcam, UK), AKT (Abcam, UK), CaMKII (Abcam, UK), CREB (Abcam, UK) and ERK1/2 (Abcam, UK) were used at 1:1000 dilutions. The dark room film development method was used to obtain images of the protein bands, which were quantified using ImageJ 1.80 software. An HP LaserJet pro MFP m126a scanner was used for film scanning, and the scanned images were analyzed via Microsoft Word software for simple color saturation and overall brightness adjustment of the image. The protein abundance was normalized to that of GAPDH.

Statistical analysis. The data are shown as the means and standard deviation ($\bar{X} \pm S$). The interaction effects were analyzed by a 2×2 factorial design. The 2.856 GHz microwave exposure and 1.5 GHz microwave exposure were regarded as two factors in the factorial design. Two-way ANOVA and multiple comparisons were performed with SPSS 19.0 software, and $^{\Delta}p < 0.05$ or $^{\Delta\Delta}p < 0.01$ were considered significant interaction effects. If interaction effects were observed, then a regression analysis was used to determine which factor played a more important role. Factors with larger absolute values of the standardized regression coefficient (β value) were considered to be of greater importance. If there were significant main effects in the anova, the posthoc multiple comparisons were conducted by the bonferroni analysis, with $^*p < 0.05$ or $^{**}p < 0.01$ (vs. C), $^{\#}p < 0.05$ or $^{\#\#}p < 0.01$ (L vs. S).

Results

Acute impairment of spatial memory abilities after 2.856 GHz and 1.5 GHz microwave exposure. The average escape latency (AEL) indicates the time needed for the rats to find the platform in the MWM. A prolonged AEL indicates a decline in spatial memory abilities.

After two days of training before microwave exposure, there were no differences in AEL between the C, S, L and SL groups, which indicated the same basic learning and memory abilities of the four groups before microwave exposure. Compared to that in the C group, the AEL of the rats in the S ($p = 0.012$), L ($p = 0.049$) and SL groups ($p = 0.001$) significantly increased 6 h after microwave exposure (Fig. 1).

No significant differences were found between the S and L groups.

No significant differences were found between the single-exposure groups (S, L) and the cumulative group (SL).

Factorial analysis of the four groups (C, S, L and SL) revealed no significant interaction effects between the 2.856 GHz and 1.5 GHz microwave radiation ($p = 0.273$). According to the standardized regression coefficient (β value) of the regression analysis, 2.856 GHz microwave radiation played major roles in the changes in AEL ($\beta_S = 0.511$, $\beta_L = 0.335$, $|\beta_S| > |\beta_L|$).

Acute inhibition of EEG after 2.856 GHz and 1.5 GHz microwave exposure. EEG examinations were performed 6 h after microwave exposure, and the EEG waveform is shown in Fig. 2A. The frequency of the EEG decreased significantly in the S ($p = 0.000$), L ($p = 0.001$) and SL ($p = 0.000$) groups ($p < 0.01$) compared with the C group (Fig. 2B). The power amplitudes of the α waves significantly decreased in the S ($p = 0.000$),

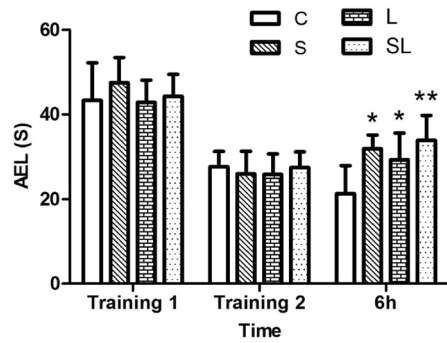


Figure 1. The AELs of the rats during the MWM test. The data are presented as the means \pm SDs. * $p < 0.05$ and ** $p < 0.01$, compared to the C group. “C” stands for the control group, “S” stands for the 2.856 GHz microwave exposure group, “L” stands for the 1.5 GHz microwave exposure group, and “SL” stands for the 2.856 and 1.5 GHz cumulative exposure group.

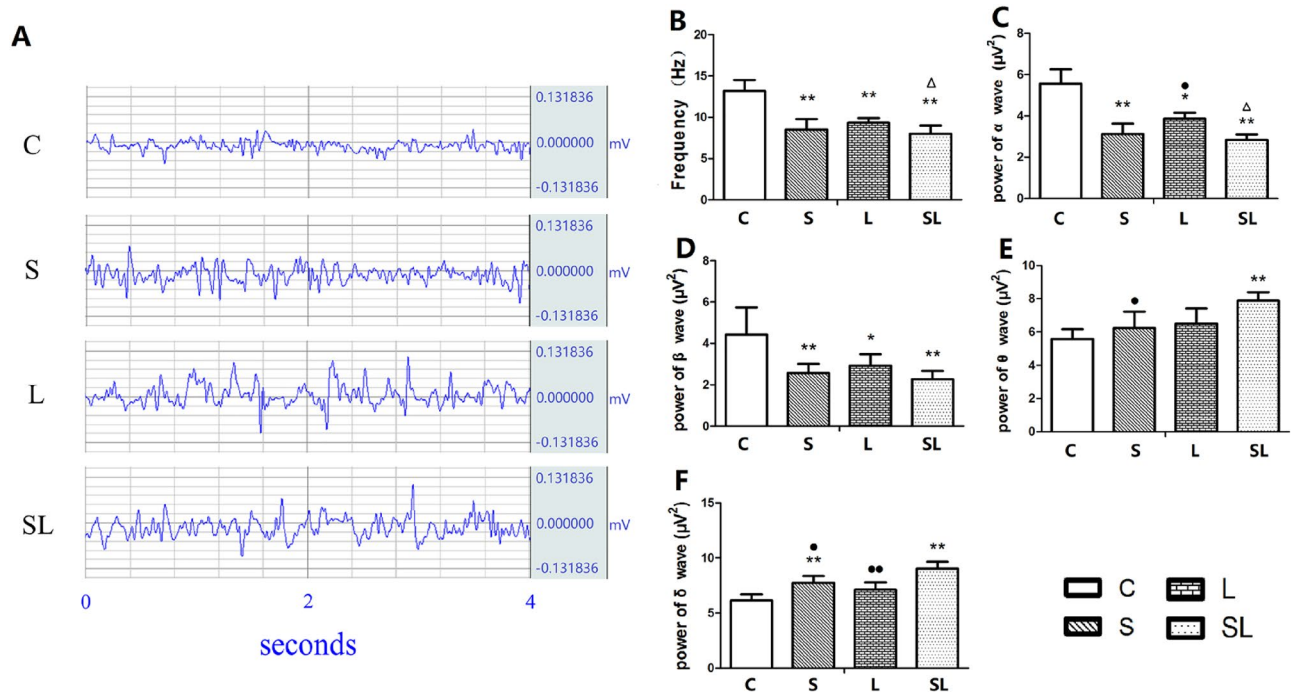


Figure 2. Changes in the frequency and power of α , β , θ and δ waves in the EEGs. The data are presented as the means \pm SDs. (A) shows the waveforms of the EEGs in the four groups. (B) shows the statistical results of the EEG frequency. (C)–(F) show the statistical results of the powers of α , β , θ and δ waves, respectively. * $p < 0.05$ and ** $p < 0.01$ compared to the C group. 1. * $p < 0.05$ and ** $p < 0.01$ compared to the cumulative group. $\Delta p < 0.05$ indicates the existence of interaction effects between the 2.856 GHz and 1.5 GHz microwaves. “C” stands for the control group, “S” stands for the 2.856 GHz microwave exposure group, “L” stands for the 1.5 GHz microwave exposure group, and “SL” stands for the 2.856 and 1.5 GHz cumulative exposure group.

L ($p = 0.002$) and SL ($p = 0.000$) groups compared with the C group, and the power amplitudes of the β waves significantly decreased in the S ($p = 0.019$), L ($p = 0.046$) and SL ($p = 0.009$) groups compared with the C group (Fig. 2C,D). The power amplitudes of the θ waves in the SL ($p = 0.007$) group and δ waves in the S ($p = 0.008$) and SL ($p = 0.000$) groups significantly increased compared with those in the C group (Fig. 2E,F).

No significant changes were found between the S and L groups.

The power amplitude of the α wave significantly increased in the L group ($p = 0.045$) compared with the SL group (Fig. 2B). The power amplitude of the θ wave in the S group was lower than that in the SL group ($p = 0.032$) (Fig. 2E). The power amplitudes of the δ waves significantly decreased in the S ($p = 0.023$) and L ($p = 0.004$) groups compared with the SL group (Fig. 2F).

Factorial analysis of the four groups (C, S, L and SL) revealed significant interaction effects between the 2.856 GHz and 1.5 GHz microwaves for the frequency changes in the EEG ($p = 0.018$) and the power amplitude

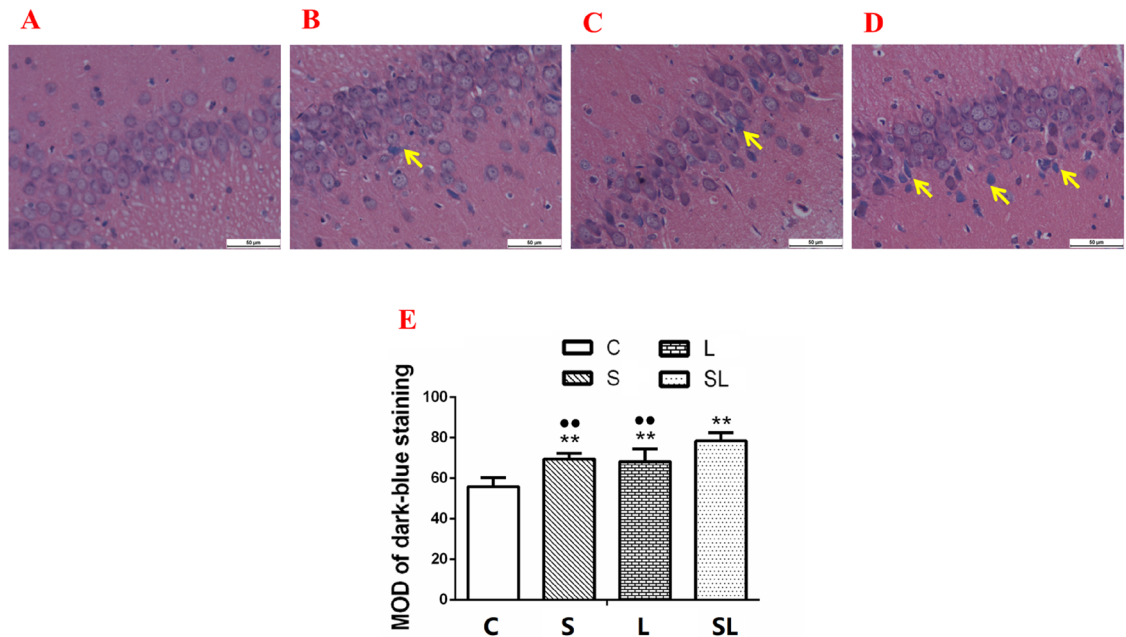


Figure 3. Pathological injuries in the hippocampus of rats 6 h after 2.856 GHz and 1.5 GHz microwave exposure. The microstructures were detected by LM 6 h after exposure to support the behavioral results. (A–D) Hippocampi of the C group, S group, L group and SL group. (E) Statistical analysis results of the MOD of dark blue staining in hippocampi. Compared to the C group, $**p < 0.01$. Compared to the cumulative group, $**p < 0.01$. There was no neuron degeneration detected by A and E., and injuries that included karyopyknosis, an irregular arrangement of cells, cell edema, and a broadening pericellular space were found in (B–D). Most injuries occurred in (D). (H&E, scale bar = 50 μ m). “C” stands for the control group, “S” stands for the 2.856 GHz microwave exposure group, “L” stands for the 1.5 GHz microwave exposure group, and “SL” stands for the 2.856 and 1.5 GHz cumulative exposure group. The data are presented as the means \pm SDs.

changes in the α wave ($p = 0.031$). According to the standardized regression coefficient (β value) of the regression analysis, 2.856 GHz microwave radiation played major roles in the changes in EEG frequency ($\beta_S = -0.69$, $\beta_L = -0.458$, $|\beta_S| > |\beta_L|$) and the power of the α wave ($\beta_S = -0.747$, $\beta_L = -0.435$, $|\beta_S| > |\beta_L|$). These results indicated that 2.856 GHz microwave radiation played major roles in the changes in the EEG for the cumulative exposure group.

Exposure to 2.856 GHz and 1.5 GHz microwaves caused significant structural injuries in the hippocampus. To assess morphological changes in neurons, histological examinations of the hippocampus were carried out. Obvious injuries in the DG areas of the hippocampus were found in the microwave exposure groups (S, L and SL) compared with the C group (Fig. 3A–D). The injuries included karyopyknosis and cell edema, as shown by the dark blue-stained nuclei. Therefore, we analyzed the dark blue areas using statistical methods. The MOD of the dark blue area of the nuclei increased significantly in the hippocampus in the S ($p = 0.000$), L ($p = 0.000$) and SL ($p = 0.000$) groups compared with the C group (Fig. 3E). The MOD of the dark blue areas of the hippocampus decreased significantly in the S ($p = 0.004$) and L ($p = 0.003$) groups compared with the SL group, which indicated that the most significant injuries occurred in the cumulative group (Fig. 3E). There were no significant interactions after the factorial analysis. According to the standardized regression coefficient (β value) of the regression analysis, 2.856 GHz microwave radiation played major roles in the changes in MOD of dark blue-stained nuclei of hippocampus ($\beta_S = 0.729$, $\beta_L = 0.621$, $|\beta_S| > |\beta_L|$).

Exposure to 2.856 GHz and 1.5 GHz microwaves induced cell apoptosis in the hippocampus. To evaluate changes in neuronal cells, apoptosis was analyzed by TUNEL staining 6 h after microwave exposure. Deep-dyed nuclei were observed in the DG area of the hippocampi in the S, L and SL groups, which indicates the occurrence of apoptosis in neurons (Fig. 4A–D). The integrated optical density (IOD) of DAB staining in the hippocampus increased significantly in the S ($p = 0.000$), L ($p = 0.000$) and SL ($p = 0.000$) groups compared with the C group (Fig. 4E). The IOD of DAB staining in the hippocampus decreased significantly in the S ($p = 0.022$) and L ($p = 0.013$) groups compared with the SL group (Fig. 4E). Factorial analysis revealed significant interaction effects in the hippocampus and cortex between the 2.856 GHz microwave radiation and 1.5 GHz microwave radiation ($p = 0.002$) groups (Fig. 4E). According to the standardized regression coefficients (β value) of the regression analysis, 1.5 GHz microwave radiation played major roles in IOD value changes in the hippocampus ($\beta_S = -0.61$, $\beta_L = -0.666$, $|\beta_S| < |\beta_L|$) and ($\beta_S = 0.544$, $\beta_L = 0.603$, $|\beta_S| < |\beta_L|$), respectively) (Fig. 4E). These results indicated that cell apoptosis occurred in the hippocampus and that 1.5 GHz microwave exposure played major roles in the changes in the cumulative exposure group.

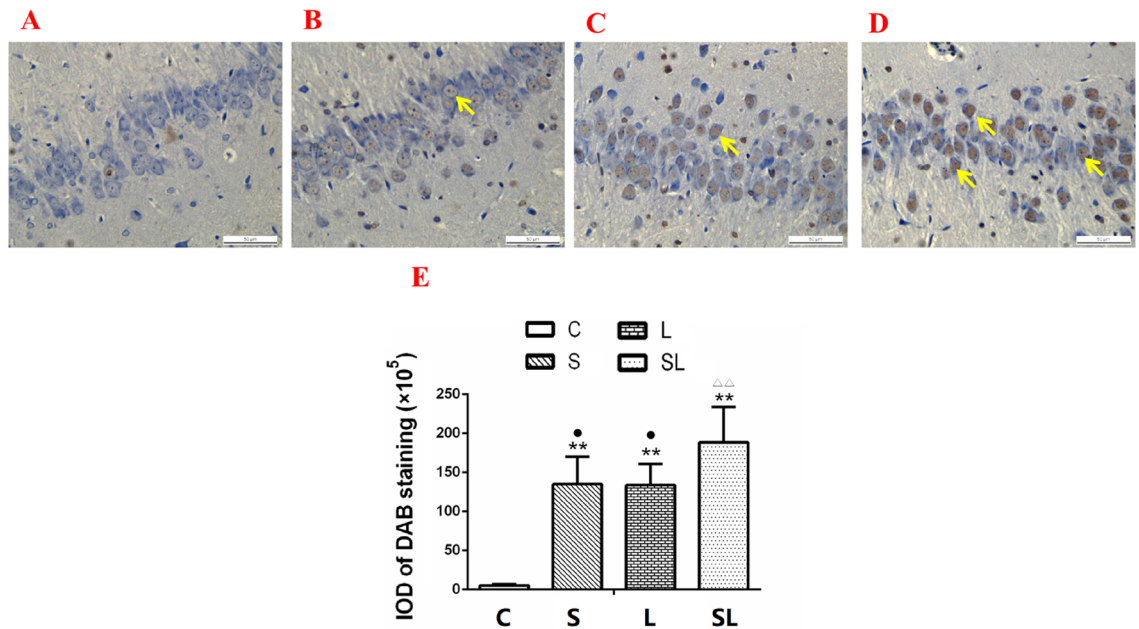


Figure 4. Cell apoptosis in the hippocampus of rats 6 h after 2.856 GHz and 1.5 GHz microwave exposures, as detected by TUNEL staining. (A–D) Hippocampi of the C group, S group, L group and SL group (TUNEL, scale bar = 50 μ m). (E) IOD changes in the hippocampus. Compared to the C group, ** $p < 0.01$. Compared to the cumulative group, ^{ΔΔ} $p < 0.01$ indicates the existence of interaction effects between the 2.856 GHz and 1.5 GHz microwaves. “C” stands for the control group, “S” stands for the 2.856 GHz microwave exposure group, “L” stands for the 1.5 GHz microwave exposure group, and “SL” stands for the 2.856 and 1.5 GHz cumulative exposure group. The data are presented as the means \pm SDs.

Changes in CREB-related signaling proteins after 2.856 GHz and 1.5 GHz microwave exposure. Six hours after microwave exposure, p-AKT/AKT ($p = 0.015$), p-CREB/CREB ($p = 0.001$) (Fig. 5A,B,D) and p-ERK/ERK ($p = 0.011$) (Fig. 6A,B) decreased significantly in the SL group, and the expression of p-CaMKII/CaMKII decreased significantly in the S ($p = 0.009$) and SL ($p = 0.000$) groups compared with the C group.

Significant differences were also found between the S and L groups. The expression of p-CaMKII/CaMKII increased significantly in the L group ($p = 0.021$) compared with the S group.

The expression of p-AKT/AKT increased significantly in the L group compared with the SL group ($p = 0.024$). The expression levels of p-CaMKII/CaMKII increased significantly in the S ($p = 0.006$) and L ($p = 0.000$) groups compared with the SL group (Fig. 5A–C). The expression levels of p-CREB/CREB increased significantly in the S ($p = 0.013$) and L ($p = 0.001$) groups compared with the SL group (Fig. 5A,D). The expression of p-ERK increased significantly in the S group ($p = 0.007$) compared with the SL group (Fig. 6A,B).

Factorial analysis of the four groups (C, S, L and SL) revealed significant interaction effects between the 2.856 GHz and 1.5 GHz microwaves only for p-CREB/CREB ($p = 0.046$) expression. According to the standardized regression coefficient (β value) of the regression analysis, the 2.856 GHz microwaves played major roles in the decreased expression of p-AKT/AKT ($\beta_S = -8.33$, $\beta_L = -0.417$, $|\beta_S| > |\beta_L|$), p-CaMKII/CaMKII ($\beta_S = -8.845$, $\beta_L = -0.396$, $|\beta_S| > |\beta_L|$) and p-CREB/CREB ($\beta_S = -0.757$, $\beta_L = -0.326$, $|\beta_S| > |\beta_L|$) (Fig. 5). According to the standardized regression coefficient (β value) of the regression analysis, the 1.5 GHz microwaves played major roles in the decreased expression of p-ERK/ERK ($\beta_S = -0.199$, $\beta_L = -0.751$, $|\beta_S| < |\beta_L|$) (Fig. 6).

Discussion and conclusions

Most previous studies focused on the dose-dependent biological effects of a single-frequency microwave exposure^{26,30,31}. However, with the increasingly serious microwave pollution in our living environments, people are exposed to microwaves at multiple frequencies. The energy distributions of microwaves with different frequencies in the organisms are different, and the biological effects depend on the energy distribution. Therefore, we hypothesized that the responses of organisms to microwaves of different frequencies would be different.

The cumulative group received more power than the single-frequency-exposure groups. Previous studies found dose-dependent effects of microwaves and showed that higher microwave power could lead to more severe effects^{2,28}. The effects in the cumulative exposure group (SL) were more serious than those in the single-frequency-exposure groups (S, L) in the EEG, structural injuries, and the expression of p-AKT/AKT, p-CaMKII/CaMKII, p-CREB/CREB and p-ERK/ERK, which might be due to the larger dose exposure.

The MWM test is a classic method for detecting spatial learning and memory abilities^{32,33}. Long-term exposure to 2.856 GHz microwaves prolonged the AELs in rats in a previous study⁵, but this study examined only the effects of one microwave frequency. We also found prolonged microwave-induced AELs. We also compared the effects

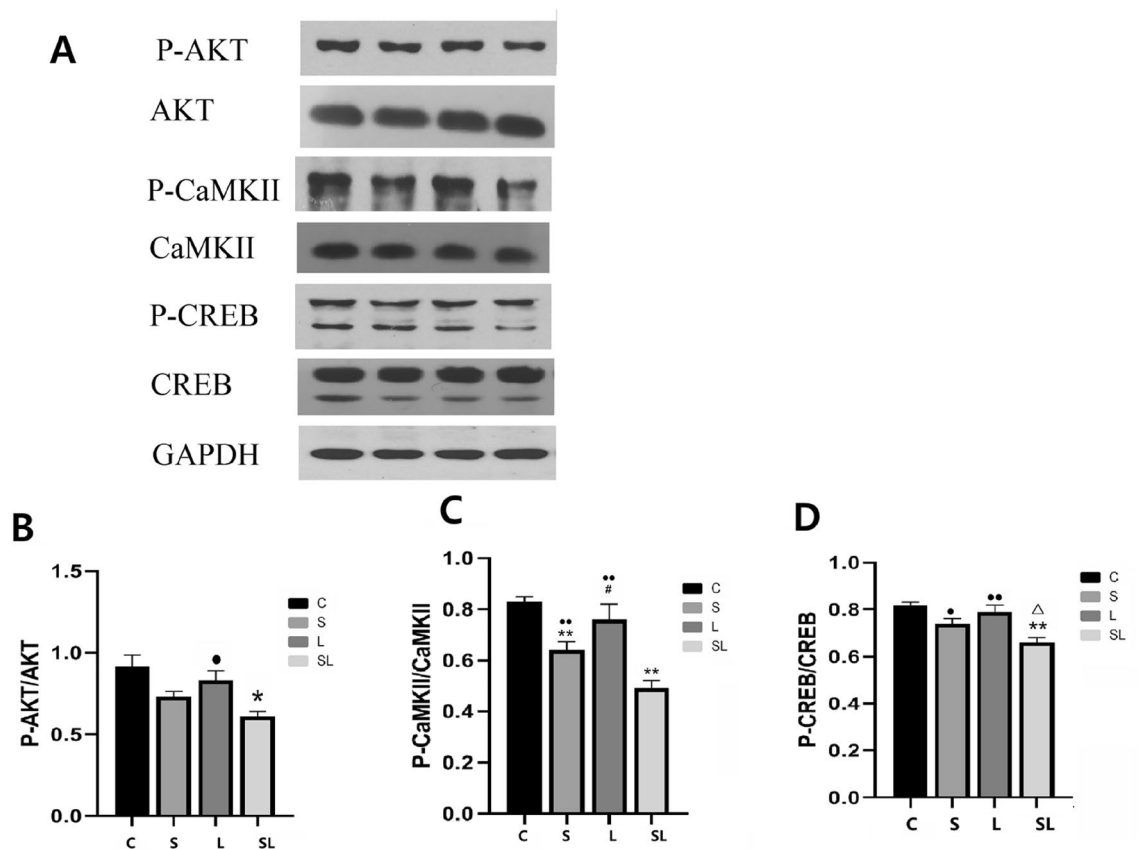


Figure 5. Comparisons of the levels of p-AKT (B), p-CaMKII (C), and p-CREB (D) in the hippocampi of the C, S, L and SL groups. (A) Expression of four proteins in the C, S, L and SL groups. (B) Statistical analysis results of p-AKT in the four groups. (C) Statistical analysis results of p-CaMKII in the four groups. (D) Statistical analysis results of p-CREB in the four groups. The data are presented as the means \pm SDs. * $p < 0.05$ and ** $p < 0.01$ compared to the C group. # $p < 0.05$ compared to the S10 group. * $p < 0.05$ and ** $p < 0.01$ compared to the cumulative group. [△] $p < 0.05$ indicates the existence of interaction effects between the 2.856 GHz and 1.5 GHz microwaves. “C” stands for the control group, “S” stands for the 2.856 GHz microwave exposure group, “L” stands for the 1.5 GHz microwave exposure group, and “SL” stands for the 2.856 and 1.5 GHz cumulative exposure group.

between the 2.856 GHz and 1.5 GHz microwaves and found no differences in the AELs, which demonstrated that 2.856 GHz and 1.5 GHz could lead to decreased spatial memory abilities in Wistar rats. No differences were found between the cumulative exposure group and single-frequency-exposure groups, and no interaction effects were found by the factorial analysis of the AELs.

EEG scans directly reflect the physiological activities of the brain and are commonly used to evaluate brain function^{34,35}. Changes in EEG activity results in many degenerative brain diseases³⁶. EEG also plays important roles in the neuromodulatory balance of memory and mental illness³⁷. Thuroczy reported that local brain exposure to 4 GHz continuous waves (CW) increased the power of δ waves³⁸. Four kinds of waves, α (12–30 Hz), β (8–12 Hz), θ (4–8 Hz) and δ (1–4 Hz), lie within the EEG spectrum. The α and β waves appear in a relaxed or nervous status of the brain, and the θ and δ waves appear in a tired or sleepy state of the brain³⁹. Our results indicated that microwave exposure caused rats to enter a more tired or depressed state.

Many studies found that microwave radiation induced structural damage in brain tissue^{11,40}. The present study found tissue injuries in the 2.856 GHz and 1.5 GHz microwave exposure groups. The injuries were similar between the two single-frequency-exposure groups. The most serious injuries were observed in the cumulative exposure groups. To clarify the type of injuries, TUNEL staining was conducted. Cell apoptosis was observed in the hippocampus and cortex of the exposure groups. Previous studies found that neuroapoptosis in developing brains might cause long-term learning and memory abnormalities⁴¹. Apoptosis might explain the microwave-induced learning and memory impairments.

Analyses of the MWM, EEG, H&E staining and TUNEL staining revealed no significant differences between the 2.856 GHz microwave exposure and 1.5 GHz microwave exposure, which suggested that microwaves with frequencies in similar ranges induced similar effects. Accumulative microwave exposure induced serious changes. Therefore, dose accumulation played a more important role than single frequency microwave exposure. Notably, interaction effects were found for the changes in the EEG frequency, power amplitudes of α waves and IOD values of the TUNEL staining in the hippocampus. The standardized regression coefficients showed that the

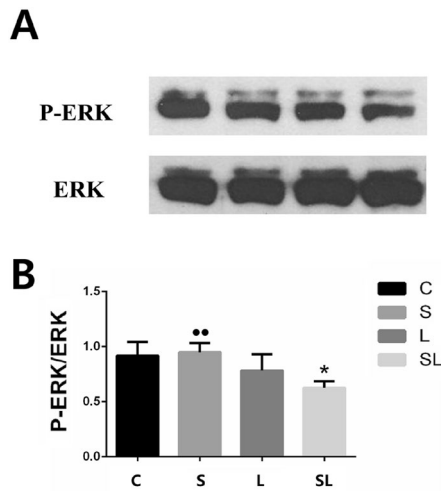


Figure 6. Comparison of the levels of p-ERK and ERK in the hippocampi of the C, S, L and SL groups. **(A)** Expression of four p-ERK and ERK proteins in the C, S, L and SL groups. **(B)** Statistical analysis results of p-ERK/ERK. The data are presented as the means \pm SDs. * $p < 0.05$. ** $p < 0.01$ compared to the cumulative group. “C” stands for the control group, “S” stands for the 2.856 GHz microwave exposure group, “L” stands for the 1.5 GHz microwave exposure group, and “SL” stands for the 2.856 and 1.5 GHz cumulative exposure group.

major factors involved in the functional and structural changes were different. For the MWM, EEG changes and p-AKT, p-CaMKII and p-CREB, The 2.856 GHz microwaves played major roles for the EEG changes, and 1.5 GHz microwave exposure played a major role in the TUNEL changes and p-ERK. The results indicated that the mechanisms of accumulative microwave exposure were complicated. The 2.856 GHz and 1.5 GHz microwaves may play different roles in the functional and structural changes of the accumulative exposure. The reasons for this result might be related to the energy and penetration depth of the microwaves.

CREB is an important transcription factor that plays an important role in the processes of learning and memory^{42–44}. The phosphorylation of CREB affects the expression or activation of genes and the overall behavior of neurons⁴⁵. Long-term facilitation alters CREB phosphorylation by increasing cAMP, which leads to the expression of related genes and ultimately results in changes in functional protein expression⁴⁶. Multiple signaling pathways, such as the PI3K/AKT pathway²¹, Ca²⁺/CaMKII pathway⁴⁷ and MEK/ERK pathway²⁰ regulate the phosphorylation of CREB. In this study, the key signaling molecules in these signaling pathways were detected. We found that the phosphorylation levels of key signaling molecules, such as p-AKT/AKT, p-CaMK II/CaMKII, p-CREB/CREB and p-ERK/ERK, were downregulated after microwave radiation.

The levels of p-AKT, p-CaMK II and p-ERK are closely related to synaptic functions. Lee et al. reported that activation of the PI3K/Akt/mTOR pathway promoted dendritic spine formation and excitatory synapse development in hippocampal neurons^{48,49}. Zhao et al.⁵⁰ found that decreased AKT phosphorylation contributed to hippocampal neuronal apoptosis in rats. The decreased p-AKT level after microwave exposure in the present study might be related to microwave-induced neuronal apoptosis. Mohajerani et al. found that the activated MAPK/ERK pathway led to transcriptional regulation and new protein synthesis in postsynaptic neurons⁵¹. Curtis et al. found that genes regulated by CREB or other transcription factor targets of the CaMK and ERK pathways mediated important adaptive responses to changes in synaptic activity, such as changes in synaptic strength and the regulation of neuronal survival and death⁵². Therefore, we concluded that the decreased p-AKT/AKT, p-CaMKII/CaMKII and p-ERK/ERK levels resulted in a decrease in synaptic function and learning and memory functions. The decreased p-CREB/CREB levels might be the result of the inhibition of these three pathways.

In terms of the molecular level, differences in the expression of p-CaMKII/CaMKII between 2.856 GHz and 1.5 GHz were found, which suggests the different sensitivities of the signal pathways to microwaves with different frequencies. Interaction effects of the two microwave frequencies were found for the changes in p-CREB/CREB. The accumulative exposure of the 2.856 GHz and 1.5 GHz microwaves aggravated the downregulation of p-CREB/CREB. Previous studies used combined exposure to communication microwaves (849 MHz and 1.95 GHz), but none of these studies analyzed the interaction effects^{53–56}.

The present study provides new insights into the biological effects of microwave radiation. Microwaves affect multiple metabolic pathways, and the frequency played an important role in the biological effects. The results related to frequency-dependent effects suggested that microwave safety standards should be based on the frequency. Past safety standards were primarily based on radiation power, and radiation frequency was defined only in a rough range⁵⁷. The interaction effects suggested that the biological effects caused by electromagnetic waves were much more complicated than previously thought. More attention should be given to this field.

Received: 21 December 2020; Accepted: 26 May 2021

Published online: 11 June 2021

References

- Kesari, K. K., Siddiqui, M. H., Meena, R., Verma, H. N. & Kumar, S. Cell phone radiation exposure on brain and associated biological systems. *Indian J. Exp. Biol.* **51**, 187–200 (2013).
- Wang, H. *et al.* Impairment of long-term potentiation induction is essential for the disruption of spatial memory after microwave exposure. *Int. J. Radiat. Biol.* **89**, 1100–1107. <https://doi.org/10.3109/09553002.2013.817701> (2013).
- Pall, M. L. Microwave frequency electromagnetic fields (EMFs) produce widespread neuropsychiatric effects including depression. *J. Chem. Neuroanat.* **75**, 43–51. <https://doi.org/10.1016/j.jchemneu.2015.08.001> (2016).
- Qiao, S. *et al.* Reduction of phosphorylated synapsin I (ser-553) leads to spatial memory impairment by attenuating GABA release after microwave exposure in Wistar rats. *PLoS ONE* **9**, e95503. <https://doi.org/10.1371/journal.pone.0095503> (2014).
- Wang, H. *et al.* Long term impairment of cognitive functions and alterations of NMDAR subunits after continuous microwave exposure. *Physiol. Behav.* **181**, 1–9. <https://doi.org/10.1016/j.physbeh.2017.08.022> (2017).
- Vorhees, C. V. & Williams, M. T. Morris water maze: procedures for assessing spatial and related forms of learning and memory. *Nat. Protoc.* **1**, 848–858 (2006).
- Kumlin, T. *et al.* Mobile phone radiation and the developing brain: Behavioral and morphological effects in juvenile rats. *Radiat. Res.* **168**, 471–479 (2007).
- Wang, B. & Lai, H. Acute exposure to pulsed 2450-MHz microwaves affects water-maze performance of rats. *Bioelectromagnetics* **21**, 52–56 (2000).
- Sharma, A., Sisodia, R., Bhatnagar, D. & Saxena, V. K. Spatial memory and learning performance and its relationship to protein synthesis of Swiss albino mice exposed to 10 GHz microwaves. *Int. J. Radiat. Biol.* **90**, 29 (2014).
- Hinrikus, H., Parts, M., Lass, J. & Tuulik, V. Changes in human EEG caused by low level modulated microwave stimulation. *Bioelectromagnetics* **25**, 431–440. <https://doi.org/10.1002/bem.20010> (2004).
- Li, H. J. *et al.* Alterations of cognitive function and 5-HT system in rats after long term microwave exposure. *Physiol. Behav.* **140**, 236–246. <https://doi.org/10.1016/j.physbeh.2014.12.039> (2015).
- Suhhova, A., Bachmann, M., Karai, D., Lass, J. & Hinrikus, H. Effect of microwave radiation on human EEG at two different levels of exposure. *Bioelectromagnetics* **34**, 264–274. <https://doi.org/10.1002/bem.21772> (2013).
- Zuo, H. *et al.* Neural cell apoptosis induced by microwave exposure through mitochondria-dependent caspase-3 pathway. *Int. J. Med. Sci.* **11**, 426–435. <https://doi.org/10.7150/ijms.6540> (2014).
- Cho, W. H. & Han, J. S. Differences in the flexibility of switching learning strategies and CREB phosphorylation levels in prefrontal cortex, Dorsal Striatum and Hippocampus in two inbred strains of mice. *Front. Behav. Neurosci.* **10**, 176. <https://doi.org/10.3389/fnbeh.2016.00176> (2016).
- Pulimood, N. S., Rodrigues, W. D. S. J., Atkinson, D. A., Mooney, S. M. & Medina, A. E. The role of CREB, SRF, and MEF2 in activity-dependent neuronal plasticity in the visual cortex. *J. Neurosci.* **37**, 6628–6637. <https://doi.org/10.1523/JNEUROSCI.0766-17.2017> (2017).
- Wang, L. *et al.* Regulation of CREB functions by phosphorylation and sumoylation in nervous and visual systems. *Curr. Mol. Med.* **16**, 885–892. <https://doi.org/10.2174/1566524016666161223110106> (2017).
- Gascon, S., Ortega, F. & Gotz, M. Transient CREB-mediated transcription is key in direct neuronal reprogramming. *Neurogenesis* **4**, e1285383. <https://doi.org/10.1080/23262133.2017.1285383> (2017).
- Ladeira, B. S. *et al.* Activity-independent effects of CREB on neuronal survival and differentiation during mouse cerebral cortex development. *Cereb. Cortex* <https://doi.org/10.1093/cercor/bhw387> (2016).
- Bao, Y. *et al.* The Neuroprotective effect of liraglutide is mediated by glucagon-like peptide 1 receptor-mediated activation of cAMP/PKA/CREB pathway. *Cell. Physiol. Biochem.* **36**, 2366–2378. <https://doi.org/10.1159/000430199> (2015).
- Jeong, S. G. & Cho, G. W. The tubulin deacetylase sirtuin-2 regulates neuronal differentiation through the ERK/CREB signaling pathway. *Biochem. Biophys. Res. Commun.* **482**, 182–187. <https://doi.org/10.1016/j.bbrc.2016.11.031> (2017).
- Liu, X., Wang, X. & Lu, J. Tenuifoliside A promotes neurite outgrowth in PC12 cells via the PI3K/AKT and MEK/ERK/CREB signaling pathways. *Mol. Med. Rep.* **12**, 7637–7642. <https://doi.org/10.3892/mmr.2015.4397> (2015).
- Xi, Y. D. *et al.* Genistein inhibits Abeta25-35-induced synaptic toxicity and regulates CaMKII/CREB pathway in SH-SY5Y cells. *Cell. Mol. Neurobiol.* **36**, 1151–1159. <https://doi.org/10.1007/s10571-015-0311-6> (2016).
- Zhao, L. *et al.* Upregulation of HIF-1alpha via activation of ERK and PI3K pathway mediated protective response to microwave-induced mitochondrial injury in neuron-like cells. *Mol. Neurobiol.* **50**, 1024–1034. <https://doi.org/10.1007/s12035-014-8667-z> (2014).
- Caraglia, M. *et al.* Electromagnetic fields at mobile phone frequency induce apoptosis and inactivation of the multi-chaperone complex in human epidermoid cancer cells. *J. Cell. Physiol.* **204**, 539–548. <https://doi.org/10.1002/jcp.20327> (2005).
- Li, P. *et al.* N-Cadherin-mediated activation of PI3K/Akt-GSK-3beta signaling attenuates nucleus pulposus cell apoptosis under high-magnitude compression. *Cell. Physiol. Biochem.* **44**, 229–239. <https://doi.org/10.1159/000484649> (2017).
- Xiong, L. *et al.* Microwave exposure impairs synaptic plasticity in the rat Hippocampus and PC12 cells through over-activation of the NMDA receptor signaling pathway. *Biomed. Environ. Sci.* **28**, 13–24. <https://doi.org/10.3967/bes2015.002> (2015).
- Kapri-Pardes, E. *et al.* Activation of signaling cascades by weak extremely low frequency electromagnetic fields. *Cell. Physiol. Biochem.* **43**, 1. <https://doi.org/10.1159/000481977> (2017).
- Tan, S. *et al.* Study on dose-dependent, frequency-dependent, and accumulative effects of 1.5 GHz and 2.856 GHz microwave on cognitive functions in Wistar rats. *Sci. Rep.* **7**, 10781. <https://doi.org/10.1038/s41598-017-11420-9> (2017).
- D'Hooge, R. & De Deyn, P. P. Applications of the Morris water maze in the study of learning and memory. *Brain Res. Rev.* **36**, 60–90 (2001).
- Inoue, S. *et al.* Microwave irradiation induces neurite outgrowth in PC12m3 cells via the p38 mitogen-activated protein kinase pathway. *Neurosci. Lett.* **432**, 35–39. <https://doi.org/10.1016/j.neulet.2007.12.002> (2008).
- Shahin, S., Banerjee, S., Swarup, V., Singh, S. P. & Chaturvedi, C. M. 2.45 GHz Microwave radiation impairs hippocampal learning and spatial memory: Involvement of local stress mechanism induced suppression of iGluR/ERK/CREB signaling. *Toxicol. Sci.* <https://doi.org/10.1093/toxsci/kfx221> (2017).
- Ning, H. *et al.* Effects of haloperidol, nanzapine, ziprasidone, and PHA-543613 on spatial learning and memory in the Morris water maze test in naive and MK-801-treated mice. *Brain Behav.* **7**, e00764. <https://doi.org/10.1002/brb3.764> (2017).
- Ahmadi, M., Rajaei, Z., Hadjzadeh, M. A., Nemati, H. & Hosseini, M. Crocin improves spatial learning and memory deficits in the Morris water maze via attenuating cortical oxidative damage in diabetic rats. *Neurosci. Lett.* **642**, 1–6. <https://doi.org/10.1016/j.neulet.2017.01.049> (2017).
- Geist, P. A., Dulka, B. N., Barnes, A., Totty, M. & Datta, S. BDNF heterozygosity is associated with memory deficits and alterations in cortical and hippocampal EEG power. *Behav. Brain Res.* **332**, 154–163. <https://doi.org/10.1016/j.bbr.2017.05.039> (2017).
- Wiegand, I. *et al.* EEG correlates of visual short-term memory as neuro-cognitive endophenotypes of ADHD. *Neuropsychologia* **85**, 91–99. <https://doi.org/10.1016/j.neuropsychologia.2016.03.011> (2016).
- Han, Y., Wang, K., Jia, J. & Wu, W. Changes of EEG Spectra and Functional Connectivity during an Object-Location Memory Task in Alzheimer's Disease. *Front. Behav. Neurosci.* **11**, 107. <https://doi.org/10.3389/fnbeh.2017.00107> (2017).
- Vakalopoulos, C. The EEG as an index of neuromodulator balance in memory and mental illness. *Front. Neurosci.* **8**, 63. <https://doi.org/10.3389/fnins.2014.00063> (2014).

38. Thuroczy, G., Kubinyi, G., Bodo, M., Bakos, J. & Szabo, L. D. Simultaneous response of brain electrical activity (EEG) and cerebral circulation (REG) to microwave exposure in rats. *Rev. Environ. Health* **10**, 135–148 (1994).
39. Karamacoska, D., Barry, R. J. & Steiner, G. Z. Resting state intrinsic EEG impacts on go stimulus-response processes. *Psychophysiology* **54**, 894–903. <https://doi.org/10.1111/psyp.12851> (2017).
40. Wang, L. F. *et al.* Microwave-induced structural and functional injury of hippocampal and PC12 cells is accompanied by abnormal changes in the NMDAR-PSD95-CaMKII pathway. *Pathobiology* **82**, 181–194. <https://doi.org/10.1159/000398803> (2015).
41. Zhong, Y. *et al.* PKA-CREB-BDNF signaling pathway mediates propofol-induced long-term learning and memory impairment in hippocampus of rats. *Brain Res.* <https://doi.org/10.1016/j.brainres.2018.04.022> (2018).
42. Zheng, C. X. *et al.* Electroacupuncture Ameliorates Learning and Memory and Improves Synaptic Plasticity via Activation of the PKA/CREB Signaling Pathway in Cerebral Hypoperfusion. *Evid.-Based Complement. Altern. Med. eCAM* **2016**, 7893710. <https://doi.org/10.1155/2016/7893710> (2016).
43. Rajan, K. E., Thangaleela, S. & Balasundaram, C. Spatial learning associated with stimulus response in goldfish *Carassius auratus*: relationship to activation of CREB signalling. *Fish Physiol. Biochem.* **41**, 685–694. <https://doi.org/10.1007/s10695-015-0038-9> (2015).
44. Middei, S. *et al.* CREB is necessary for synaptic maintenance and learning-induced changes of the AMPA receptor GluA1 subunit. *Hippocampus* **23**, 488–499. <https://doi.org/10.1002/hipo.22108> (2013).
45. Deisseroth, K., Bito, H. & Tsien, R. W. Signaling from synapse to nucleus: postsynaptic CREB phosphorylation during multiple forms of hippocampal synaptic plasticity. *Neuron* **16**, 89–101 (1996).
46. Yin, J. C. & Tully, T. CREB and the formation of long-term memory. *Curr. Opin. Neurobiol.* **6**, 264–268 (1996).
47. Guo, Y., Lv, Q., Zou, X. Q., Yan, Z. X. & Yan, Y. X. Mechanical strain regulates osteoblast proliferation through Ca²⁺-CaMK-CREB signal pathway. *Chin. Med. Sci. J. Chung-kuo i hsueh kò hsueh tsa chih* **31**, 100–106 (2016).
48. Xuan, F. & Jian, J. Epigallocatechin gallate exerts protective effects against myocardial ischemia/reperfusion injury through the PI3K/Akt pathway-mediated inhibition of apoptosis and the restoration of the autophagic flux. *Int. J. Mol. Med.* **38**, 328–336. <https://doi.org/10.3892/ijmm.2016.2615> (2016).
49. Lee, C. C., Huang, C. C. & Hsu, K. S. Insulin promotes dendritic spine and synapse formation by the PI3K/Akt/mTOR and Rac1 signaling pathways. *Neuropharmacology* **61**, 867–879. <https://doi.org/10.1016/j.neuropharm.2011.06.003> (2011).
50. Zhao, Y. *et al.* Reduced AKT phosphorylation contributes to endoplasmic reticulum stress-mediated hippocampal neuronal apoptosis in rat recurrent febrile seizure. *Life Sci.* **153**, 153–162. <https://doi.org/10.1016/j.lfs.2016.04.008> (2016).
51. Mohajerani, M. H., Sivakumaran, S., Zacchi, P., Aguilera, P. & Cherubini, E. Correlated network activity enhances synaptic efficacy via BDNF and the ERK pathway at immature CA3 CA1 connections in the hippocampus. *Proc. Natl. Acad. Sci. USA* **104**, 13176–13181. <https://doi.org/10.1073/pnas.0704533104> (2007).
52. Curtis, J. & Finkbeiner, S. Sending signals from the synapse to the nucleus: possible roles for CaMK, Ras/ERK, and SAPK pathways in the regulation of synaptic plasticity and neuronal growth. *J. Neurosci. Res.* **58**, 88–95 (1999).
53. Lee, H. J. *et al.* Lymphoma development of simultaneously combined exposure to two radiofrequency signals in AKR/J mice. *Bioelectromagnetics* **32**, 485–492. <https://doi.org/10.1002/bem.20655> (2011).
54. Lee, H. J. *et al.* The effects of simultaneous combined exposure to CDMA and WCDMA electromagnetic fields on rat testicular function. *Bioelectromagnetics* **33**, 356–364. <https://doi.org/10.1002/bem.20715> (2012).
55. Kim, H. N. *et al.* Analysis of the cellular stress response in MCF10A cells exposed to combined radio frequency radiation. *J. Radiat. Res.* **53**, 176–183 (2012).
56. Jin, Y. B. *et al.* Effects of simultaneous combined exposure to CDMA and WCDMA electromagnetic fields on serum hormone levels in rats. *J. Radiat. Res.* **54**, 430–437. <https://doi.org/10.1093/jrr/rrs120> (2013).
57. Patrick Reilly, J. Human exposure standards in the frequency range 1 Hz To 100 kHz: the case for adoption of the IEEE standard. *Health Phys.* **107**, 343–350. <https://doi.org/10.1097/HP.0000000000000112> (2014).

Acknowledgements

This study was financed by the National Natural Science Foundation of China (Grant 61401497) and the National Natural Science Foundation of China (Grant 31570847).

Author contributions

S.T., H.W. and R.P. conceived the experiments and designed the study. H.Z. conducted the microwave irradiation. X.X. conducted the EEG and image analysis. L.Z., J.Z., B.Y., H.W., Y.H., J.D. and Y.G. analyzed the MWM, EEG, and WB data. S.T. wrote the manuscript.

Competing interests

The authors declare no competing interests.

Additional information

Correspondence and requests for materials should be addressed to H.W. or R.P.

Reprints and permissions information is available at www.nature.com/reprints.

Publisher's note Springer Nature remains neutral with regard to jurisdictional claims in published maps and institutional affiliations.



Open Access This article is licensed under a Creative Commons Attribution 4.0 International License, which permits use, sharing, adaptation, distribution and reproduction in any medium or format, as long as you give appropriate credit to the original author(s) and the source, provide a link to the Creative Commons licence, and indicate if changes were made. The images or other third party material in this article are included in the article's Creative Commons licence, unless indicated otherwise in a credit line to the material. If material is not included in the article's Creative Commons licence and your intended use is not permitted by statutory regulation or exceeds the permitted use, you will need to obtain permission directly from the copyright holder. To view a copy of this licence, visit <http://creativecommons.org/licenses/by/4.0/>.

© The Author(s) 2021